

Supplement of Biogeosciences, 17, 4663–4679, 2020
<https://doi.org/10.5194/bg-17-4663-2020-supplement>
© Author(s) 2020. This work is distributed under
the Creative Commons Attribution 4.0 License.



Supplement of

Sediment release of dissolved organic matter to the oxygen minimum zone off Peru

Alexandra N. Loginova et al.

Correspondence to: Anja Engel (aengel@geomar.de)

The copyright of individual parts of the supplement might differ from the CC BY 4.0 License.

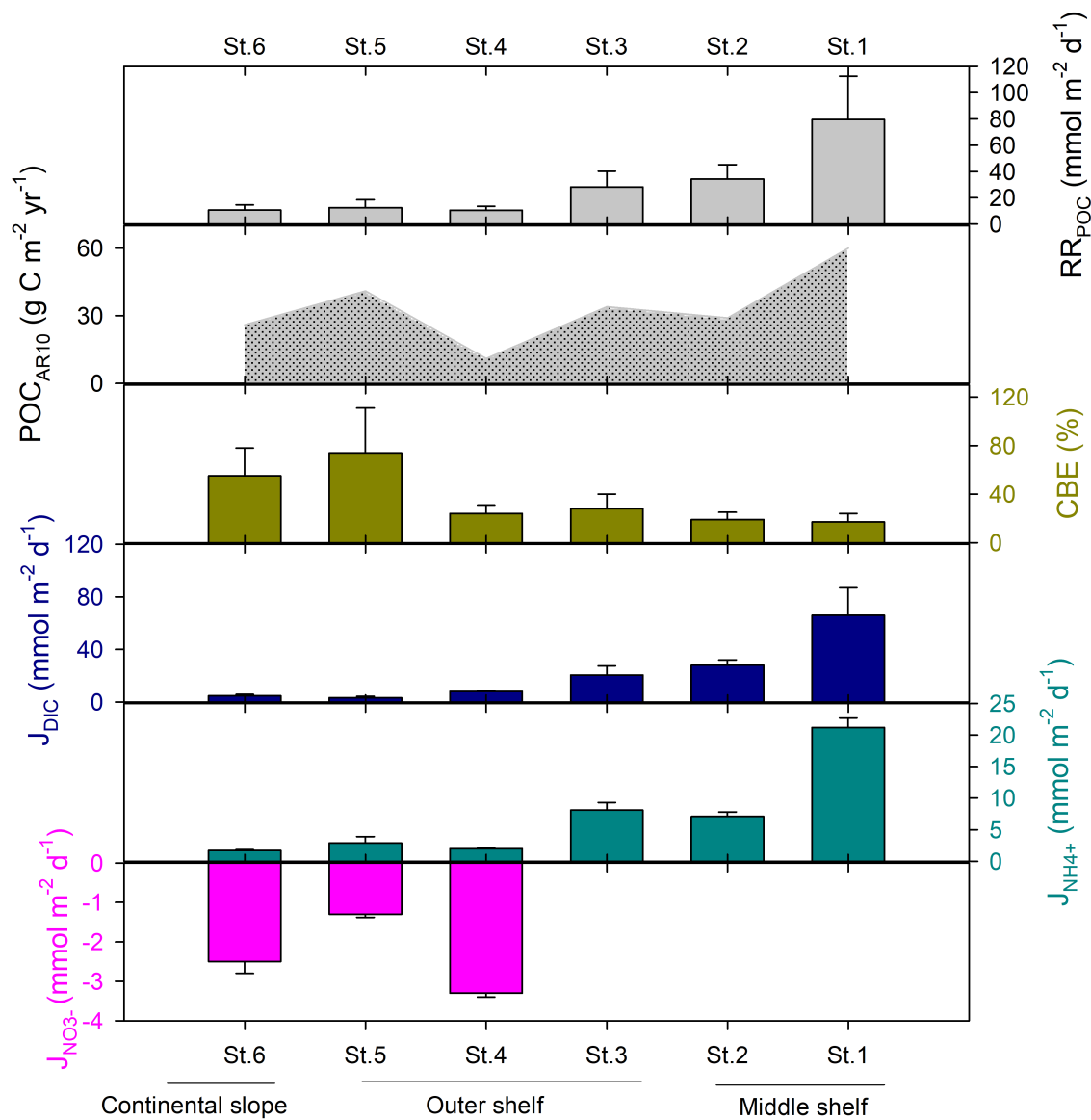


Figure S1. POC rain rates (RR_{POC}), POC accumulation rate at 10 cm (POC_{AR10}), carbon burial efficiency at 10 cm (CBE), and benthic DIC flux (J_{DIC}) previously published by Dale et al. (2015) and benthic NH_4^+ flux ($J_{NH_4^+}$) and benthic NO_3^- flux ($J_{NO_3^-}$) previously published by Sommer et al. (2016) for the studied area.

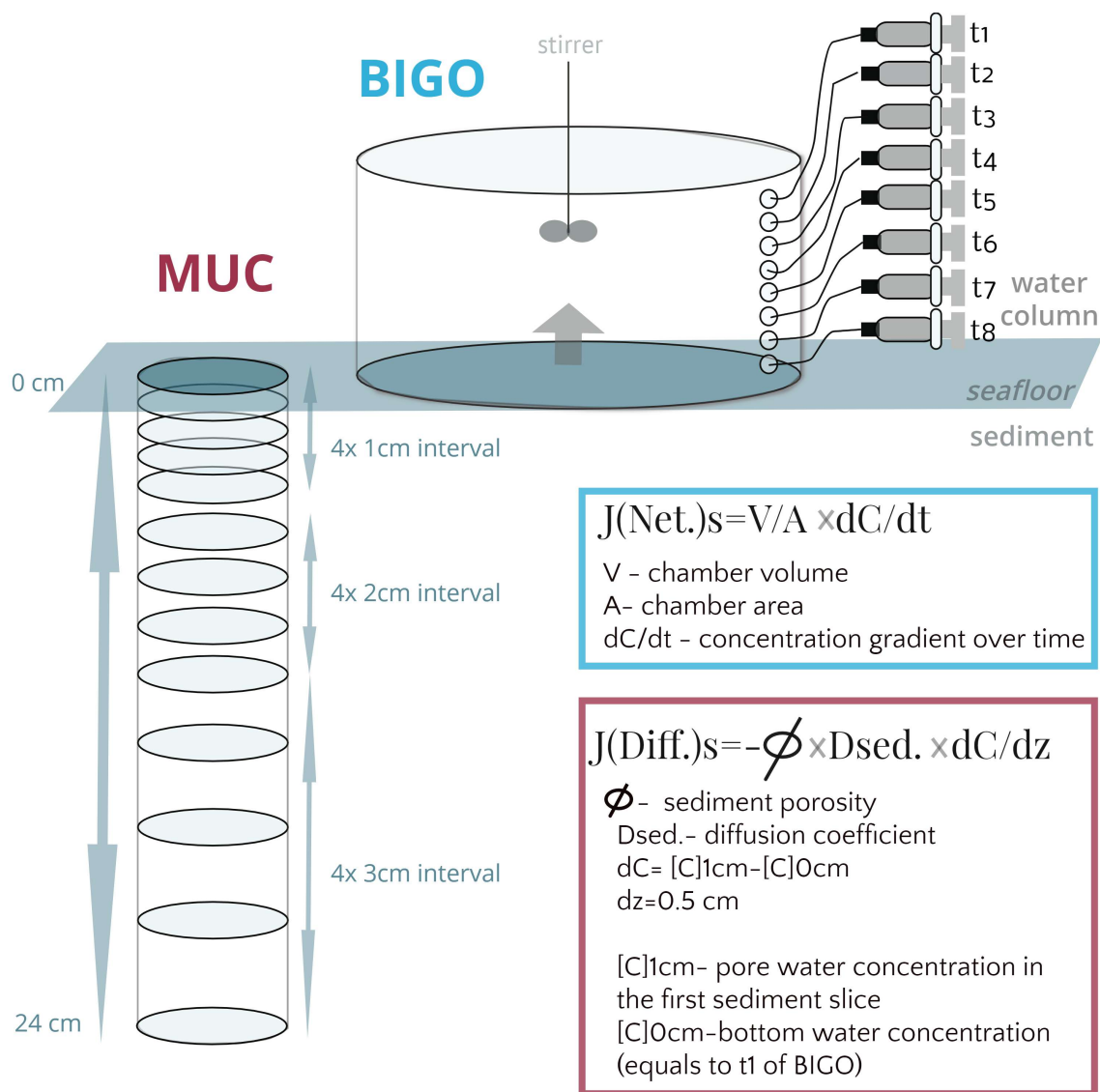


Figure S2. Schematic representation of a sediment core taken by MUC and a BIGO chamber. Each sediment core was sliced over 1–3 cm intervals to get average resolution of 12 samples per sediment core. A concentration gradient of solutes was obtained as a difference of the porewater concentration of a solute, analysed at the first sediment slice and bottom water solute concentration, that was assumed equal to the solute concentration measured in the corresponding BIGO chamber at time-point t_1 . Each BIGO chamber was deployed over the period of ~ 32 hrs, during that time samples were retrieved sequentially at time points of $\sim 0.2, 4, 9, 12, 12, 17, 25$ and ~ 30 hrs using glass air and water tight 40 ml syringes. The concentration gradient of a solute over time was obtained by fitting a linear regression to the time-concentration plot, as it is shown on Fig 3.

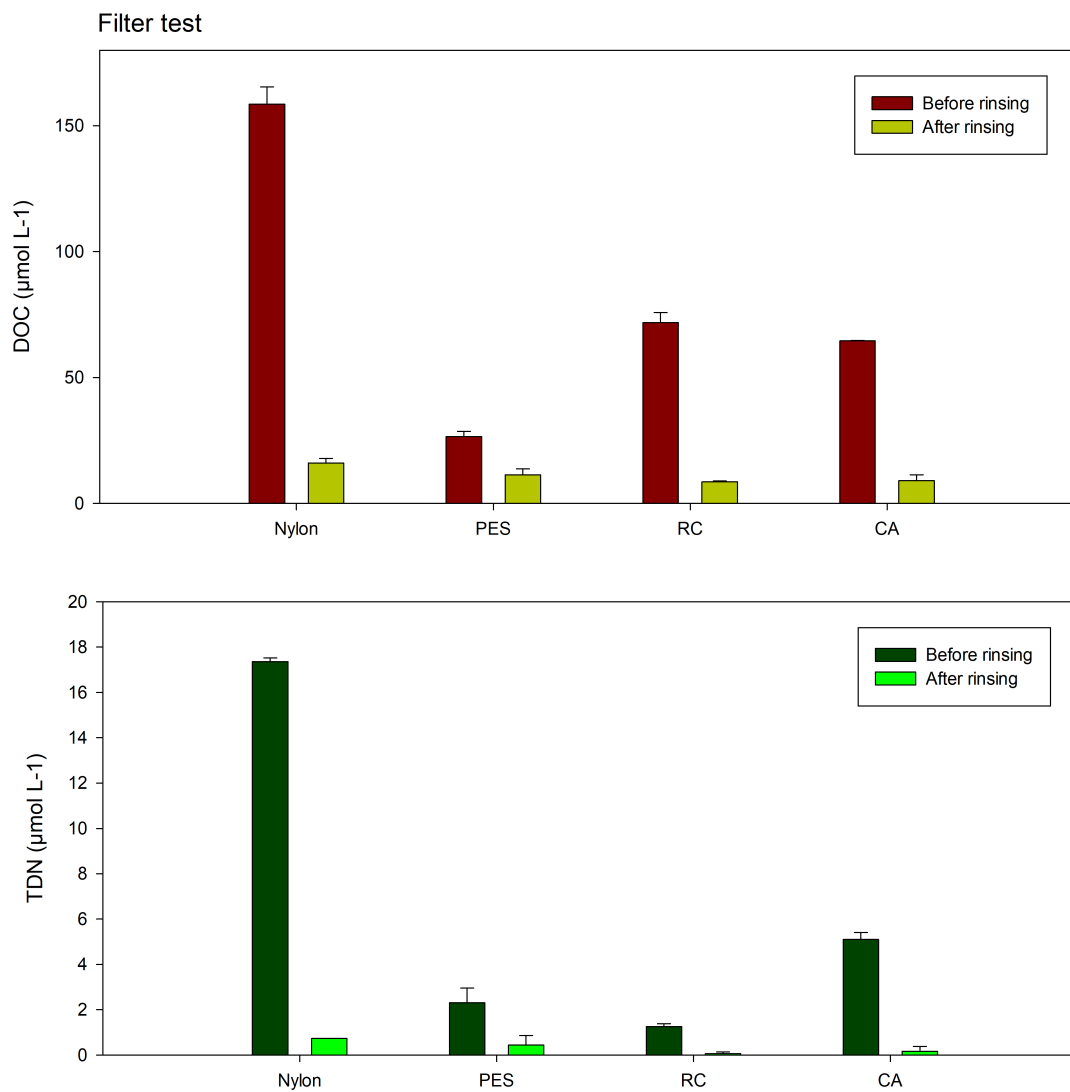
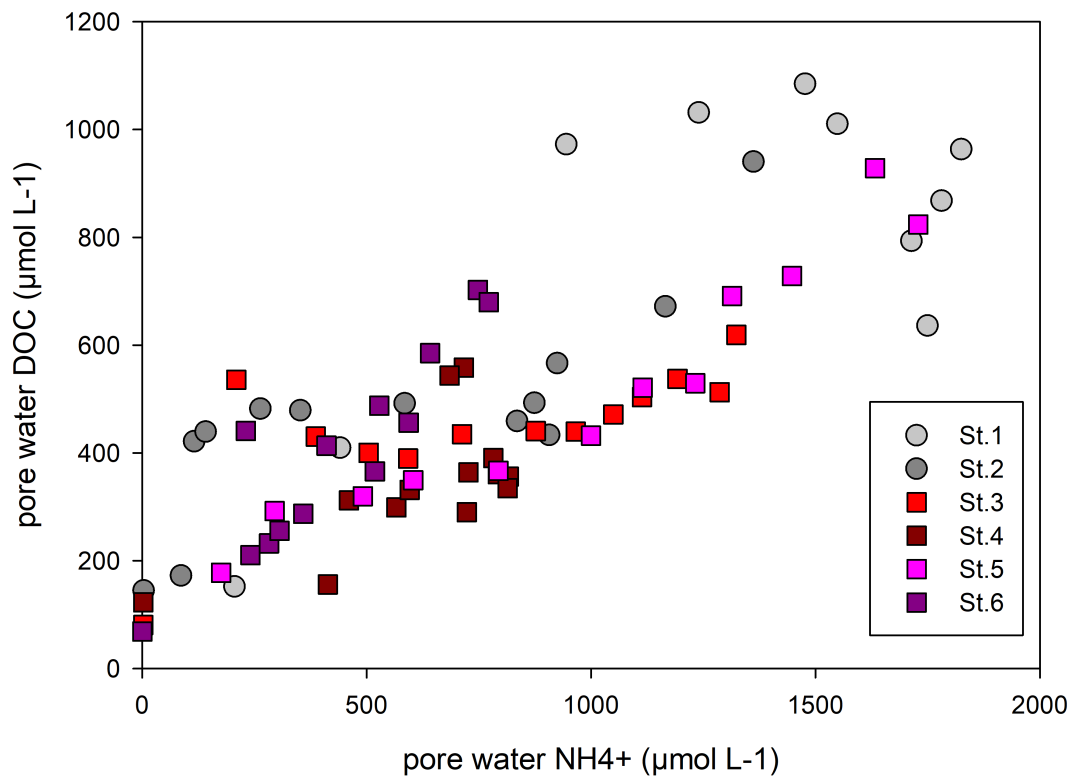
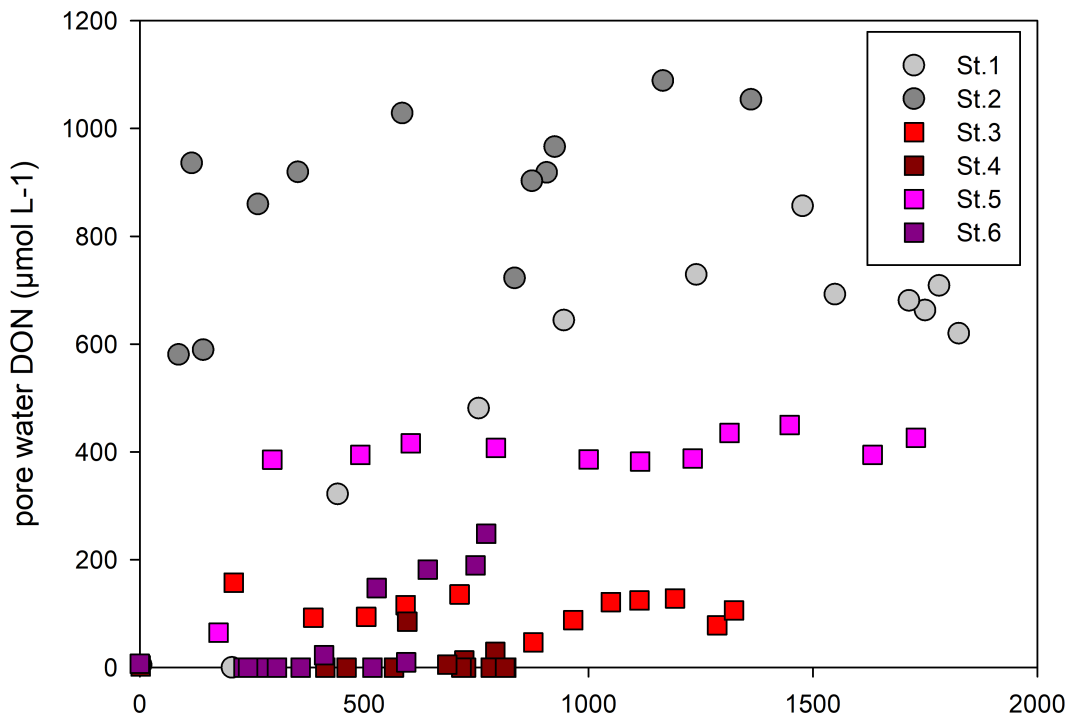


Figure S3. DOC and TDN concentrations in ultrapure water after passing through not rinsed and rinsed with 60 mL of ultrapure water nylon, polyethersulphone (PES), regenerated cellulose (RC) and cellulose acetate (CA) filters.



5

Figure S4. Concentrations of DON and DOC versus NH_4^+ in the porewater.

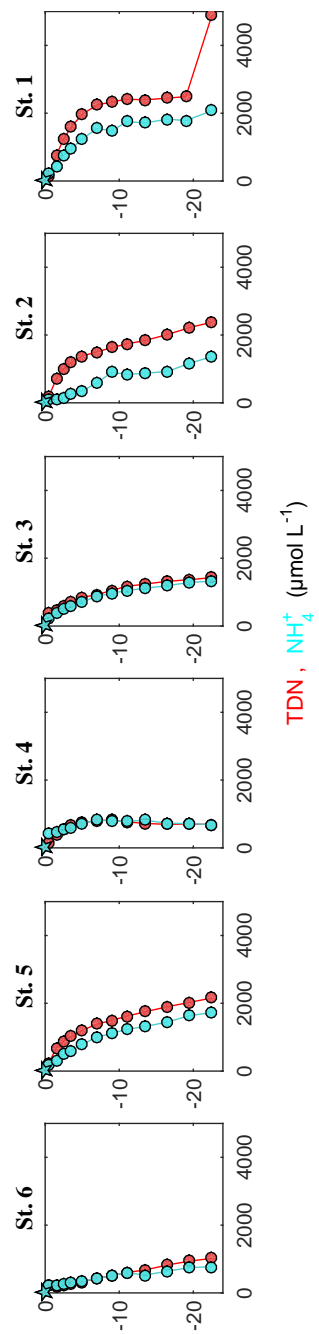


Figure S5. Concentrations of TDN and NH_4^+ measured in porewaters off Peru.

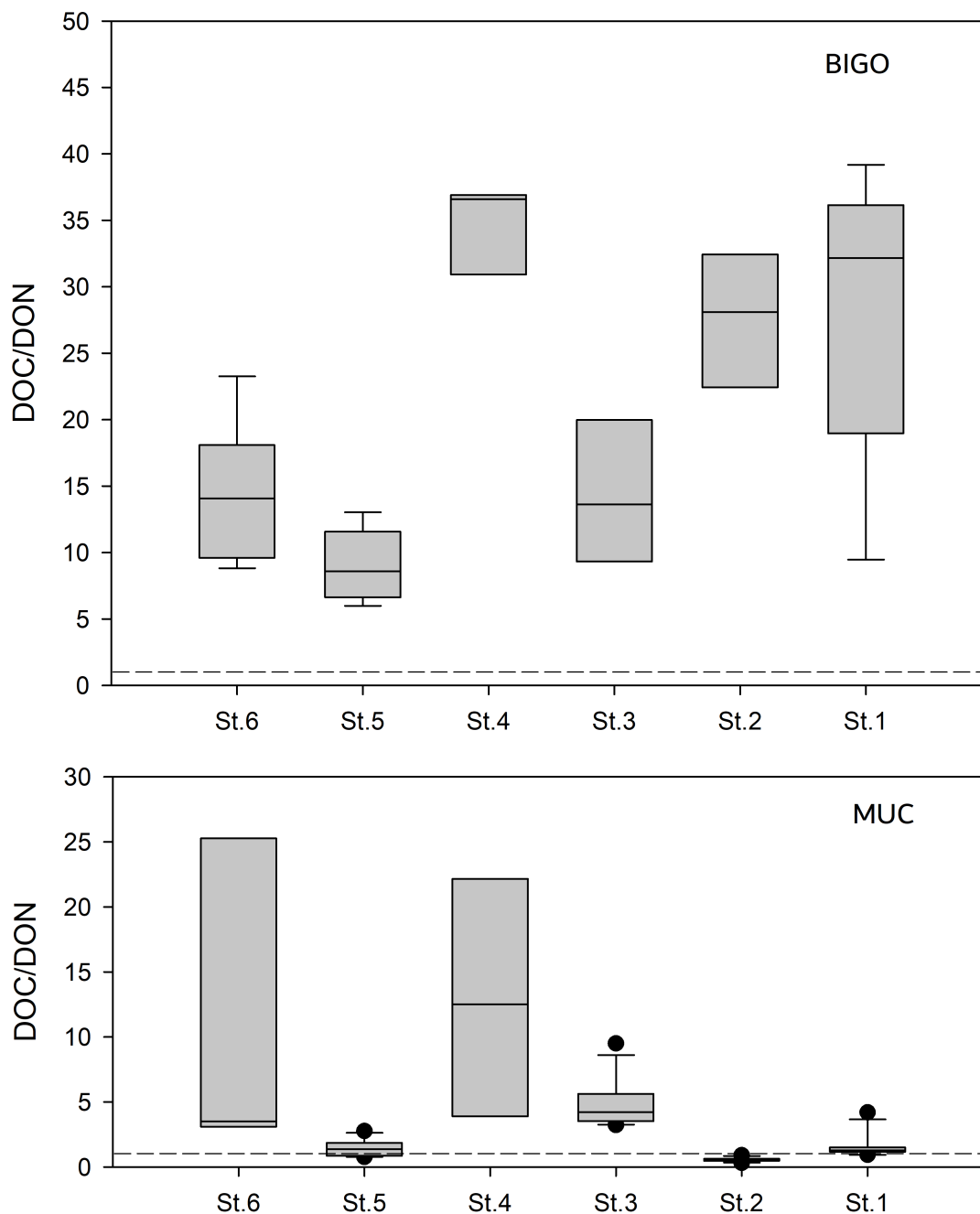


Figure S6. DOC/DON ratio in the porewaters (lower panel) and in the BIGO chambers (upper panel). All values, measured at one station are presented as one box. The DOC/DON of $\sim Inf.$ due to DON concentrations below detection were assumed as not a number and were excluded from the box plot. Horizontal line represents 1:1 DOC/DON ratio.

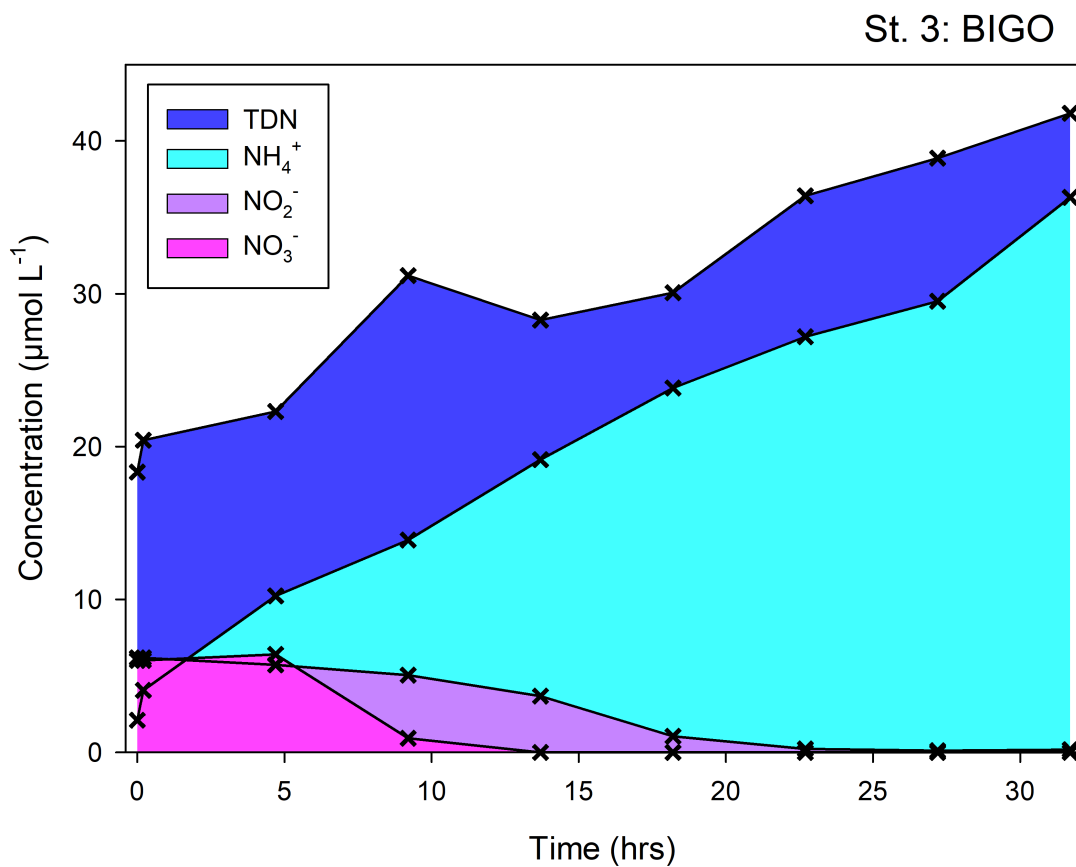


Figure S7. Concentrations of TDN, NH_4^+ , NO_2^- and NO_3^- , measured in the BIGO chamber at St.3.

Table S1. Calculated fluxes and gradients of DOC and optically active DOM components

Sampling system	Station /Parameter	$a_{CDOM}(325)^a$	$S_{275-295}^b$	Comp.1 ($\times 10^{-2}$) ^c	Comp.2 ^c	Comp.3 ^c	Comp.4 ^c
BIGO	St.1	-0.1 \pm 1.2	-0.016 \pm 0.017	2.99 \pm 0.15	0.04 \pm 0.05	-0.24 \pm 0.82	0.086 \pm 0.112
	St.2	0.06 \pm 0.16	-0.008 \pm 0.009	2.69 \pm 0.08	0.08 \pm 0.03	0.09 \pm 0.07	0.043 \pm 0.044
	St.3	-1.4 \pm 1.0	-0.013 \pm 0.009	2.72 \pm 0.04	0.07 \pm 0.02	0.05 \pm 0.23	0.046 \pm 0.024
	St.4	0.8 \pm 1.0	-0.004 \pm 0.006	0.13 \pm 0.02	0.04 \pm 0.05	-0.44 \pm 0.65	-0.005 \pm 0.039
	St.5	-0.5 \pm 1.3	-0.011 \pm 0.016	2.65 \pm 0.08	0.06 \pm 0.04	0.14 \pm 0.10	0.046 \pm 0.043
	St.6	-0.6 \pm 0.7	-0.009 \pm 0.005	2.83 \pm 0.10	0.08 \pm 0.04	0.01 \pm 0.44	0.039 \pm 0.112

(a) CDOM gradient in $m^{-1}d^{-1}$, (b) CDOM spectral slope gradient in $mm^{-1}d^{-1}$, (c) FDOM gradients in $QSE d^{-1}$.